Accepted Manuscript

Biochemical and dynamic basis for combinatorial recognition of H3R2K9me2 by dual domains of UHRF1

Suman Abhishek, M. Angel Nivya, Naveen Kumar Nakarakanti, Waghela Deeksha, Sanjeev Khosla, Eerappa Rajakumara

PII: S0300-9084(18)30097-X

DOI: 10.1016/j.biochi.2018.04.010

Reference: BIOCHI 5394

To appear in: *Biochimie*

Received Date: 24 January 2018

Accepted Date: 10 April 2018

Please cite this article as: S. Abhishek, M.A. Nivya, N.K. Nakarakanti, W. Deeksha, S. Khosla, E. Rajakumara, Biochemical and dynamic basis for combinatorial recognition of H3R2K9me2 by dual domains of UHRF1, *Biochimie* (2018), doi: 10.1016/j.biochi.2018.04.010.

UHRF1 is a multi-domain protein comprising of a tandem tudor (UHRF1 TTD), a PHD finger, and a SET and RING-associated domain. It is required for the maintenance of CG methylation, heterochromatin formation and DNA repair. Isothermal titration calorimetry binding studies of unmodified and methylated lysine histone peptides establish that the UHRF1 TTD binds dimethylated Lys9 on histone H3 (H3K9me2). Further, MD simulation and binding studies reveal that TTD-PHD of UHRF1 (UHRF1 TTD-PHD) preferentially recognizes dimethyl-lysine status. Importantly, we show that Asp145 in the binding pocket determines the preferential recognition of the dimethyl-ammonium group of H3K9me2. Interestingly, PHD finger of the UHRF1 TTD-PHD has a negligible contribution to the binding affinity for recognition of K9me2 by the UHRF1 TTD. Surprisingly, Lys4 methylation on H3 peptide has an insignificant effect on combinatorial recognition of R2 and K9me2 on H3 by the UHRF1 TTD-PHD. We propose that subtle variations of key residues at the binding pocket determine status specific recognition of histone methyl-lysines by the reader domains.

Biochemical and dynamic basis for combinatorial recognition of H3R2K9me2 by dual domains of UHRF1

Suman Abhishek[1,#], M. Angel Nivya[1,#], Naveen Kumar Nakarakanti[1,#], Waghela Deeksha[1], Sanjeev Khosla[2,*] and Eerappa Rajakumara[1,*]

[1]Department of Biotechnology, Indian Institute of Technology Hyderabad, Kandi, Sangareddy, 502285, Telangana, India

[2]Centre for DNA Fingerprinting and Diagnostics (CDFD), Hyderabad 500001, India.

[#] These authors contributed equally to this work.

[*] Corresponding authors: ER, E-mail: eraj@iith.ac.in; SK, E-mail: sanjuk@cdfd.org.in

UHRF1 is a multi-domain protein comprising of a tandem tudor (UHRF1 TTD), a PHD finger, and a SET and RING-associated domain. It is required for the maintenance of CG methylation, heterochromatin formation and DNA repair. Isothermal titration calorimetry binding studies of unmodified and methylated lysine histone peptides establish that the UHRF1 TTD binds dimethylated Lys9 on histone H3 (H3K9me2). Further, MD simulation and binding studies reveal that TTD-PHD of UHRF1 (UHRF1 TTD-PHD) preferentially recognizes dimethyl-lysine status. Importantly, we show that Asp145 in the binding pocket determines the preferential recognition of the dimethyl-ammonium group of H3K9me2. Interestingly, PHD finger of the UHRF1 TTD-PHD has a negligible contribution to the binding affinity for recognition of K9me2 by the UHRF1 TTD. Surprisingly, Lys4 methylation on H3 peptide has an insignificant effect on combinatorial recognition of R2 and K9me2 on H3 by the UHRF1 TTD-PHD. We propose that subtle variations of key residues at the binding pocket determine status specific recognition of histone methyl-lysines by the reader domains.

Keywords: UHRF1; Tandem Tudor Domains; TTD-PHD; H3K9me2 recognition; 53BP1; Isothermal Titration Calorimetry; Molecular Dynamics Simulation

Abbreviations

TTD: Tandom Tudor domain

PHD: Plant Homeodomain

TTD-PHD: Tandom Tudor domain- Plant Homeodomain

MD: Molecular dynamics

ITC: Isothermal titration calorimetry

K_D: Molar dissociation constant

Da: Dalton

Å: Angstrom

OD: Optical Density

ΔG: Binding Free Energy

1. Introduction

Methylated and unmethylated lysine and arginine residues of histone H3 and H4 are epigenetic marks in the chromatin. These epigenetic marks are recognized by a variety of reader domains present in protein modalities, including the plant homeodomain (PHD), PWWP, chromodomains, and Tandem Tudor domains (TTD) [1]. Such recognition mechanisms regulate functions of chromatin template-based biological processes including gene regulation, DNA replication, and recombination.

UHRF1 (Ubiquitin-like, containing PHD and RING finger domain 1) is also known as ICBP90 in humans and Np95 in mouse. It is a multi-domain protein comprising of an N-terminal ubiquitin-like domain (UBQ), followed by a TTD (UHRF1 TTD), a PHD (UHRF1 PHD), a SET-and-RING-associated (UHRF1 SRA) domain and a C-terminal Really Interesting New Gene (RING) domain (Fig. 1A). It is required for the maintenance of DNA Methyltransferase 1 (DNMT1) directed DNA methylation during DNA replication [2,3] and heterochromatin formation [4]. UHRF1 PHD, is previously implicated in the regulation of euchromatic transcription [5] and heterochromatin organization [6] and, is known to bind unmodified Arg2 (H3R2) of histone H3 [5,7,8].

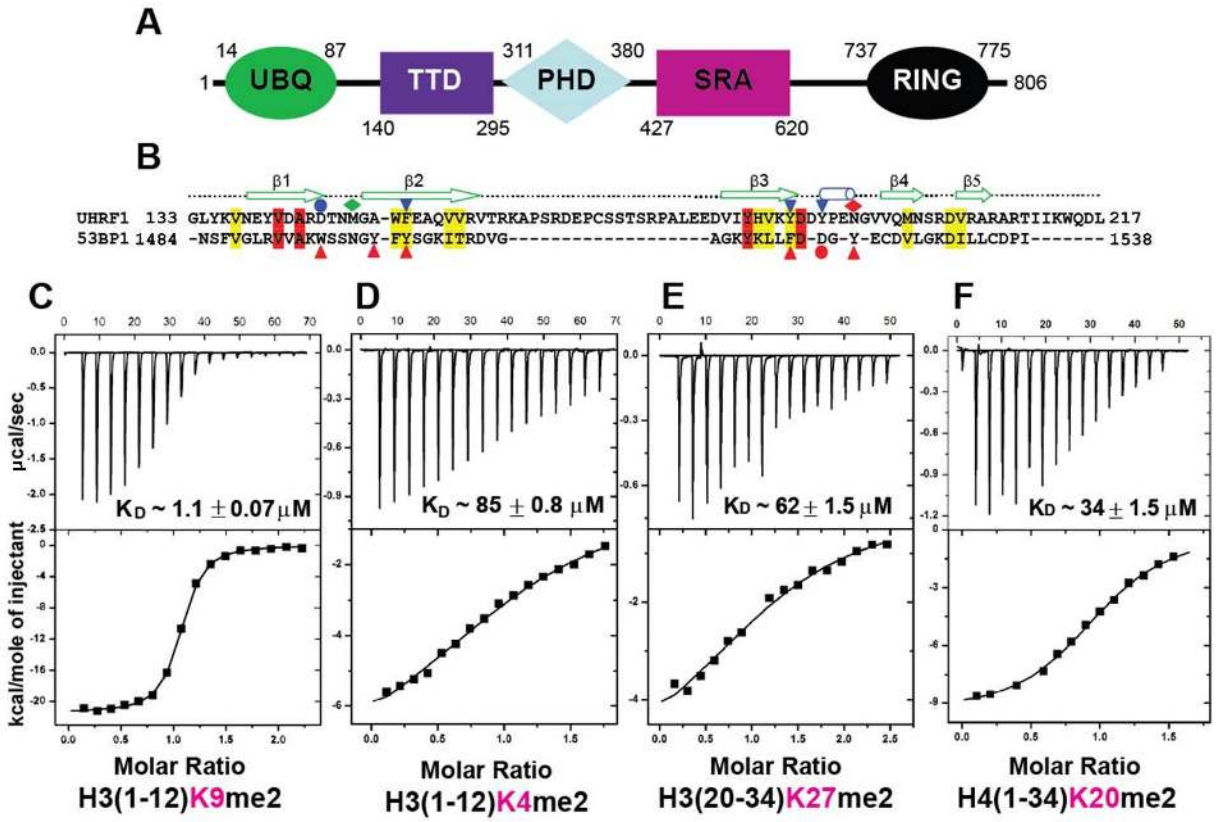

Fig. 1. Domain architecture of UHRF1, sequence alignments of its TTD with 53BP1's, and ITC binding studies of methyl-lysine histone peptides with UHRF1 TTD.

(A) Schematic representation of the domain architecture of UHRF1. (B) Sequence comparison between Tudor 1 of TTDs of UHRF1 and 53BP1. Secondary structural elements of the UHRF1 TTD are indicated above the sequences (β-strands are in green arrows and loops are in dotted lines). Residues highlighted in a background color-code correspond to their conservation level: fully-conserved, red; conservative substitutions, yellow. Residues that form the aromatic amino acid-lined cage for K9me2 recognition in UHRF1 and 53BP1 are indicated as inverted blue and red upright triangles, respectively. Filled blue and red circles designate the acidic residues, which interact with methyl-lysine in UHRF1 TTD and 53BP1 TTD, respectively. Green and red rectangles correspond to residues that form van der Waals contacts with the aliphatic and ammonium group of the K9me2 side chain in UHRF1, respectively. ITC measurements of the binding of the UHRF1 TTD to (C) H3K9me2 (D) H3K4me2 (E)

H3K27me2 (F) H4K20me2 peptides. Binding stoichiometry (N) is 1 for ITC measurements reported in Fig. 1 to 5.

In vitro, UHRF1 TTD and UHRF1 PHD show independent binding to H3K9me and H3R2 respectively [5,7–10]. Methyl-lysine residues of histone and non-histone proteins are recognized by the aromatic cage of TTDs (Fig. 1B) [11–15]. Crystal structures of the UHRF1 TTD-PHD bound to H3R2K9me3 peptide show that UHRF1 can simultaneously (also known as combinatorial) engage H3R2 and H3K9me3 on a single H3 tail through TTD and PHD linked recognition modules (Supplementary Fig. 1) [16,17], and combinatorial recognition is required for the epigenetic inheritance of DNA methylation in vivo [18,19]. The SRA domain, of the plant SUVH histone methyltransferase, recognizes 5-methylcytosine (5mC) and 5-hydroxymethyl cytosine (5hmC) in different sequence contexts and methylation statuses [20,21]. Recognition of hemi-mCG by the UHRF1 SRA leads to allosteric activation of the UHRF1 to recognize the H3R2 and H3K9me2 marks by its TTD-PHD cassette [2,3,19,22–26].

The degree of methylation (also known as methylation status) such as mono-, di- or tri- methylation on lysine residues can confer distinct functions. For instance, active promoter and transcription factor binding regions in the chromatin are commonly di- or tri-methylated (H3K4me2/3) [27,28] that also mark active transcription start sites [29,30]. Status specific read-out of methyl-lysine histone mark by the reader domain directly impact the epigenetic gene regulation. 53BP1 is recruited to chromatin regions flanking double-stranded breaks (DSBs) of DNA through the interaction of its TTD (53BP1 TTD) with H4K20me2 [11]. 53BP1 TTD shows plasticity in selective recognition of dimethyl-lysine mark on both histone and non-histone proteins [11–15]. In contrast, BPTF, the largest subunit of the ATP-dependent chromatin-remodeling complex NURF, binds tightly to H3K4me3 through its PHD finger, but weakly to H3K4me2 [31].

Different epigenetic marks on histones show substantial cross-talk that not only control a variety of physiological processes but also provide their regulatory potential [32,33]. Different histone modifications can influence each other either in a positive or negative manner through effector/reader-domain mediated readouts [32]. H3S10

phosphorylation and/ or H3K14 acetylation are required for ejection of HP1 bound to H3K9me3 and inhibition of heterochromatin formation [32]. Similarly, the H3T3 phosphorylation negatively affects the H3R2 recognition by the UHRF1 PHD and the H3R2K9me3 recognition by the UHRF1 TTD-PHD [5,16]. Combinatorial binding has also been observed for 14-3-3, UHRF1 TTD-PHD and PHD-BROMO of BPTF to H3S10phK9/14ac, H3R2K9me3 and H3K4me3H4K16ac respectively [34,35].

With this background, we have determined the binding specificity of UHRF1 TTD for methylated histone tails. This study establishes that the UHRF1 TTD exhibits higher binding affinity towards H3K9me2 compared to H3K9me1/3. In contrast, it exhibits significantly lower binding affinity towards H4K20me2. PHD finger has an insignificant contribution to the H3K9me2 recognition by the TTD of UHRF1 TTD-PHD cassette in the absence of H3R2. We have employed a computational tool, molecular dynamic (MD) simulation, to characterize the methyl status specific binding of H3R2K9me by the TTD-PHD, and to analyze the effects of H3K4 di-methylation on H3R2K9me recognition. We have validated the MD simulation data through ITC binding study. These studies establish that the UHRF1 TTD-PHD exhibits lower binding free energy (ΔG_{bind}) towards H3R2K9me2 compared to H3R2K9me3. MD simulation study also indicates that Asp145, positioned at the methyl-lysine binding pocket, determines the preferential recognition of dimethyl-lysine status over trimethyl-lysine. Further studies also reveal the insignificant effect of dimethylation of K4 on simultaneous recognition of H3R2 and H3K9me2 marks by the UHRF1 TTD-PHD cassette.

2. Material and methods

2.1 Expression and Purification of UHRF1 TTD and UHRF1 TTD-PHD

The cDNA encoding full-length human UHRF1 was obtained from Open bio-systems. We generated two different hexahistidine-SUMO tagged constructs containing UHRF1 residues 140-295 and 140-380 that correspond to the TTD and TTD-PHD, respectively. Protein was expressed in *Escherichia coli* Rosetta2 (DE3) (Novagen). Cells were grown in Luria-Bertani (LB) broth at 37ºC till OD_{600} reached 0.5-0.6, then the temperature was decreased to 20ºC and the culture was induced with 0.4 mM of isopropyl-1-thio-D-galactopyranoside (IPTG). For expression of TTD-PHD protein, the

medium was supplemented with 100μM of $ZnCl_2$, before IPTG induction. The cell cultures were grown for 15 hrs, following which cells were harvested and re-suspended in lysis buffer (25 mM Tris-HCl, pH 7.5, 500 mM NaCl, 10 mM imidazole and 3 mM β-mercaptoethanol). Cells were lysed by ultrasonic homogenizer and then the lysate was clarified by centrifugation at 40,000g for 1 hr. The hexahistidine-SUMO fusion protein was purified on a nickel-charged column (HisTrap HP, GE Healthcare). After elution with a 750 mM imidazole containing buffer, the fusion protein was cleaved with Ulp1 protease (25 U ml^{-1}) during a 16 hr dialysis step at 4 ºC. The protein was further purified by gel filtration chromatography (HiLoad Superdex 75 26/60, GE Healthcare) column, which was equilibrated with a buffer containing 15 mM Tris-HCl, pH 7.5, 50 mM NaCl, 3 mM DTT. Purified UHRF1 TTD and UHRF1 TTD-PHD were concentrated to 20 and 10 mg mL^{-1}, respectively at 4 ºC in Vivaspin 20 mL (Vivascience AG) 5,000 Da cut-off concentrators.

2.2 ITC measurements

The equilibrium molar dissociation constant (K_D), molar ratio (N) and thermodynamic parameters of the UHRF1 TTD and UHRF1 TTD-PHD bound to methylated lysine or unmethylated H3 or H4 histone peptides were determined using a VP-ITC calorimeter (MicroCal, LLC) at 25°C. The proteins were dialyzed overnight against a buffer containing 40 mM Tris-HCl, 120 mM NaCl, and 2 mM β-mercaptoethanol, pH 7.5 at 4°C. HPLC purified peptides were purchased from Yale WM Keck foundation. Lyophilized peptides were dissolved in the same buffer used for protein dialysis. The protein and peptides were used at concentrations of 100 μM to 250 μM and 1 mM to 2.5 mM, respectively. The volume of the protein in the reaction cell was 210 μL, and the reference cell was filled with deionized water. The peptide was sequentially added in 2.3 μL per injection (for a total of 15-16 injections) at 3-min intervals. The data were processed using MicroCal Origin software. The titration data were deconvoluted based on a binding model containing “one set of sites” using a nonlinear least-squares algorithm. The binding enthalpy change (ΔH), association constant (K_A), and binding stoichiometry (N) were permitted to vary, during the iterative least-squares minimization process, until the insignificant change was observed in the error function. An error function, which is reported in Supplementary table 1, is sum of

the squared deviations between the data and the model curve. The thermodynamic parameters for methylated or unmethylated lysines on H3 or H4 histone peptides binding to UHRF1 TTD and UHRF1 TTD-PHD are provided in Supplementary table 1.

2.3. MD Simulation

2.3.1. Preparation of UHRF1 TTD-PHD for simulation

The crystal structure of UHRF1 TTD-PHD complexed with H3K9me3 (PDB ID: 4GY5) [17] was prepared for simulation. Using Schrodinger's Maestro Molecular modeling suit, the H3K9me3 was modified to H3K9me2, H3K4me2K9me3 and H3K4me2K9me2 by virtually editing the methylation marks. Bond orders were assigned, and Hydrogen atoms were added followed by H-bond optimization and restrained minimization using OPLS3 force field. Protonation statuses were determined at physiological pH 7.0 using PROPKA [36,37]. All the water molecules were removed.

2.3.2. Molecular dynamics (MD) simulations

MD simulation was done for time-dependent investigations of protein-peptide interactions and conformational dynamics of studied complex systems. In the current study, we carried out MD simulations for different methylated lysine of H3 using Desmond MD simulations program [Desmond Molecular Dynamics System, Version 2.2, D.E. Shaw Research, New York, NY, 2009]. All systems were solvated in an orthorhombic box (a=b=c=10Å and $\alpha=\beta=\gamma=90^{o}$) with explicit SPC (Single Point Charge) water model. The interactions were calculated with the OPLS3 force field. The complex was neutralized in buffer system with 0.15 M NaCl. The particle-mesh Ewald method [38] was used to calculate the long-range electrostatic interactions. A cut-off radius of 9.0 Å was applied for short-range van der Waals and Coulomb interactions. The systems were simulated under an isothermal-isobaric ensemble (NPT) with the temperature of 300K and the pressure of 1 bar. Nose-Hoover thermostat [39] and Martyna–Tobias–Klein [40] methods were implemented to maintain the temperature and the pressure of the systems, respectively. A time step of 2 fs was used for the overall simulations. The systems were minimized and equilibrated with default protocols of the Desmond. Finally, 10 ns non-constrained MD simulation was performed for each system, and the coordinates were saved for every time step.

2.3.3. Protein-ligand interaction analyses

Ligand-peptide interactions are screened throughout the MD simulations. To identify the hydrogen bond, maximum distance of 3.5 Å and minimum donor angle of 120^{o} were considered. In the case of a face to face pi-pi stacking interaction, angle and distance, between the rings less than 30^{o} and less than 4.4 Å, respectively, were set.

2.3.4. Molecular Mechanics-Generalized Born Surface Area (MM-GBSA) calculations

ΔG_{bind} of the Protein-ligand interactions at 10ns of the simulation were estimated using MM-GBSA method (Prime module of the Schrodinger's molecular modeling package) [Schrödinger Release 2017-1: Prime, version 3.8, Schrödinger, LLC, New York, NY, 2014;] [41] for UHRF1 TTD-PHD with H3K9me3, H3K9me2, H3K4me2K9me3 and H3K4me2K9me2 peptides.

3. Results

3.1. UHRF1 TTD selectively recognizes the K9 methylation on histone H3

We used ITC-based binding studies to monitor the possibility of sequence-specific recognition of methyl-lysine histone peptides by UHRF1 TTD. Our binding measurements reveal that the UHRF1 TTD binds to H3(1-12)K9me2 peptide with a K_D of 1.1 μM and a stoichiometry of 1:1 (Fig. 1C). The binding is weaker to the H3(1-12)K4me2 and H3(1-12)K4me3 peptides with a K_D of 85.0 μM (Fig. 1D) and 126 μM (Supplementary table 1) respectively. Similarly, UHRF1 TTD exhibits weaker affinity to H3(20-34)K27me2 with a K_D of 62 μM (Fig. 1E). Thus, the UHRF1 TTD exhibits a higher specificity for H3K9me2 on histone H3, with 77- and 56-fold preference over H3K4me2 and H3K27me2, respectively.

Structure-based sequence comparison, of UHRF1 TTD with that of 53BP1's, indicates that residues involved in K20me recognition on histone H4 are significantly conserved in UHRF1 (Fig. 1B). Therefore, we presume that UHRF1 TTD can also recognize the H4K20me. Binding study has shown that the UHRF1 TTD binds to H4(1-34)K20me2 peptide with a K_D of 34 μM (Fig. 1F). Contrast to our assumption, UHRF1 TTD exhibits 31-fold lower affinity towards H4K20me2 compared to H3K9me2.

3.2. Methylation Status-Specific Readout of H3K9me by the UHRF1 TTD

As previously reported [16], ITC-based binding studies establish that the UHRF1 TTD binds H3(1-12)K9me3 peptide with a K_D of 5.6 μM, which is 5-fold weaker than binding to H3(1-12)K9me2 peptide (Fig. 1C and 2A). Similarly, the binding is also weaker for methylation statuses lower than dimethylation: it exhibits a K_D of 12.0 μM for a complex formation with H3(1-12)K9me1 (Fig. 2B) and a K_D of 160 μM for a complex formation with H3(1-12)K9me0 (Fig. 2C).

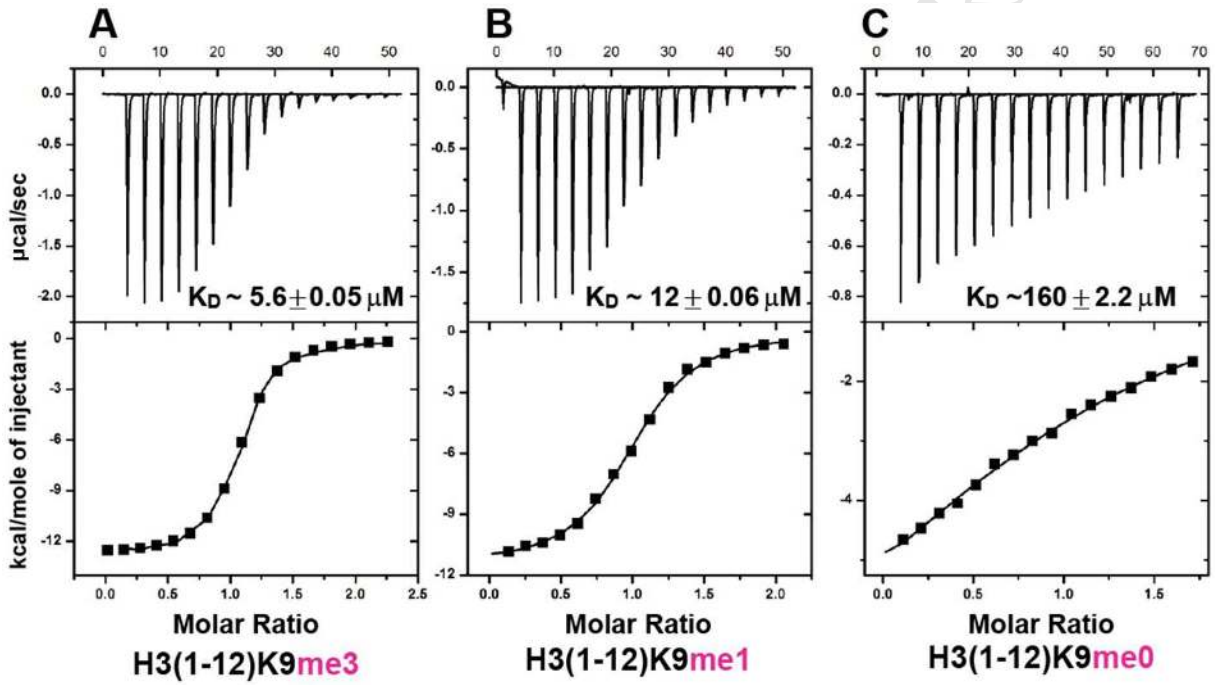

Fig. 2. Raw ITC data (upper panel) and normalized integration data (lower panel) of enthalpy plots for binding of different methyl-lysine statuses of H3K9me peptides to UHRF1 TTD. Enthalpy plots for the binding of the UHRF1 TTD to (A) H3K9me3, (B) H3K9me1 and (C) H3K9me0 peptides. The inset lists the measured molar dissociation constants.

3.3. MD simulation studies on binding of H3R2K9me2 and H3R2K9me3 peptides to UHRF1 TTD-PHD Cassette

TTD and PHD of UHRF1 are involved in combinatorial recognition of H3K9me and H3R2 marks [16]. We carried out MD simulation on, energy minimized, TTD-PHD-H3(1-12)K9me2 and TTD-PHD-H3(1-12)K9me3 complexes: (A) to capture the dynamics of TTD-PHD binding to H3R2K9me peptides in the context of different methylation statuses (B) to analyze the dynamics of binding pocket residues contribution to peptide recognition (C) to compute ΔG_{bind} of TTD-PHD to H3K9me peptides. Insignificant fluctuation of RMSDs of protein and ligand, and RMSFs of ligand indicate that both the protein TTD-PHD and the ligand methyl-lysine peptides are stable during the course of the simulation (Supplementary Fig. 2A,B and 3A,B). Overall, H3R2K9me2 and H3R2K9me3 peptides have similar network of interactions with TTD-PHD throughout the simulation (Fig. 3), and these peptides also exhibited similar conformations (Fig. 3C,D).

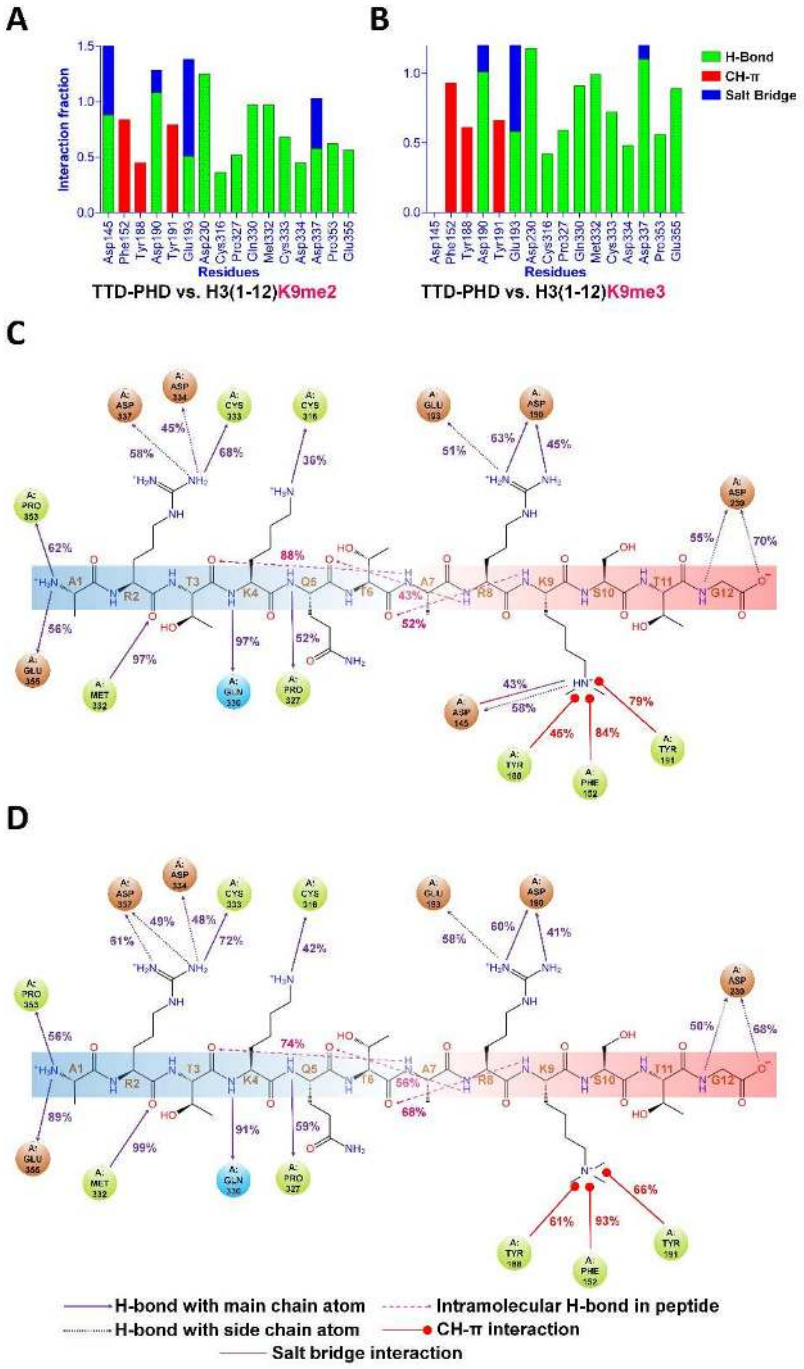

Fig. 3. Residual interaction profile of UHRF1 TTD-PHD with di- and tri-methylated lysine 9 of H3(1-12) peptide in MD simulation. Histograms display interaction fraction of protein residues during simulation time with (A) H3K9me2 and (B) H3K9me3 peptides. 2D-interaction diagrams of the protein residues contact with the (C) H3K9me2 and (D) H3K9me3 peptides. Same interaction symbols are also used in Fig. 5.

H3R2 is recognized by the negatively charged surface groove of PHD finger. Guanidinium group of Arg2 is recognized by the Asp337, Asp334 and Cys333 residues through the network of salt bridge and hydrogen bond interactions in TTD-PHD-H3R2K9me3 complex structure [5,16,17] (Supplementary Fig. 1). Above network of interactions are unaltered throughout the simulation in UHRF1-TTD PHD when complexed with H3R2K9me2 and H3R2K9me3 peptides (Fig. 3C,D).

Phe152, Tyr188 and Tyr191 residues from TTD domain of TTD-PHD form aromatic cage binding pocket that binds to K9me3 mark through hydrophobic and CH-π interactions [16,17] (Fig. 3). Through the simulation time, all aromatic residues interact with K9me3 and K9me2 of the peptides mainly through hydrophobic interactions (Fig. 3A,B). The Side chain carboxyl group of Asp145 forms a hydrogen bond interaction with dimethylammonium group of H3R2K9me2 peptide (Fig. 3A,C), which is, surprisingly, absent in H3R2K9me3 peptide (Fig. 3B,D). Another notable difference is that TTD-PHD has significantly lower ΔG_{bind} for H3R2K9me2 compared to H3R2K9m3 (Table 1) corresponding to higher binding affinity and stability of H3R2K9me2 peptide.

ΔG_{bind} of UHRF1 TTD-PHD and of mutants v/s following Peptides				
	H3R2K9me2	**H3R2K9me3**	**H3R2K4me2K9me2**	**H3R2K4me2K9me3**
UHRF1 TTD-PHD	-130.42	-111.98	-127.35	-113.34
UHRF1 TTD-PHD Asp145Glu	-137.68	-120.57		
UHRF1 TTD-PHD Asp145Ala	-109.222	-111.59		

Table1: MM/GBSA calculated ΔG_{bind} for UHRF1 TTD-PHD (receptor) bound to H3(1-12) peptide with different lysine methylation statuses.

3.4. UHRF1 TTD-PHD Cassette preferentially binds dimethyl-lysine 9 of Histone H3 peptide

An additional Asp145 mediated hydrogen bond interaction with H3K9me2 and a lower ΔG_{bind} indicate the possibility of preferential recognition of H3R2K9me2 peptide over H3R2K9me3 by the UHRF1 TTD-PHD. We have undertaken ITC binding studies of H3(1-12)K9me2 peptide by the UHRF1 TTD-PHD cassette, which exhibits K_D of 0.15

μM (Fig. 4A). By contrast, the UHRF1 TTD-PHD affinity for H3(1-12)K9me3 peptide is 6-fold weaker (K_D of 0.85 μM) compared to its affinity towards H3(1-12)K9me2 peptide (Fig. 4B). Therefore, ITC studies suggest that UHRF1 TTD-PHD recognizes both di- and tri- methylation statuses of K9 on H3, but has preference for H3K9me2.

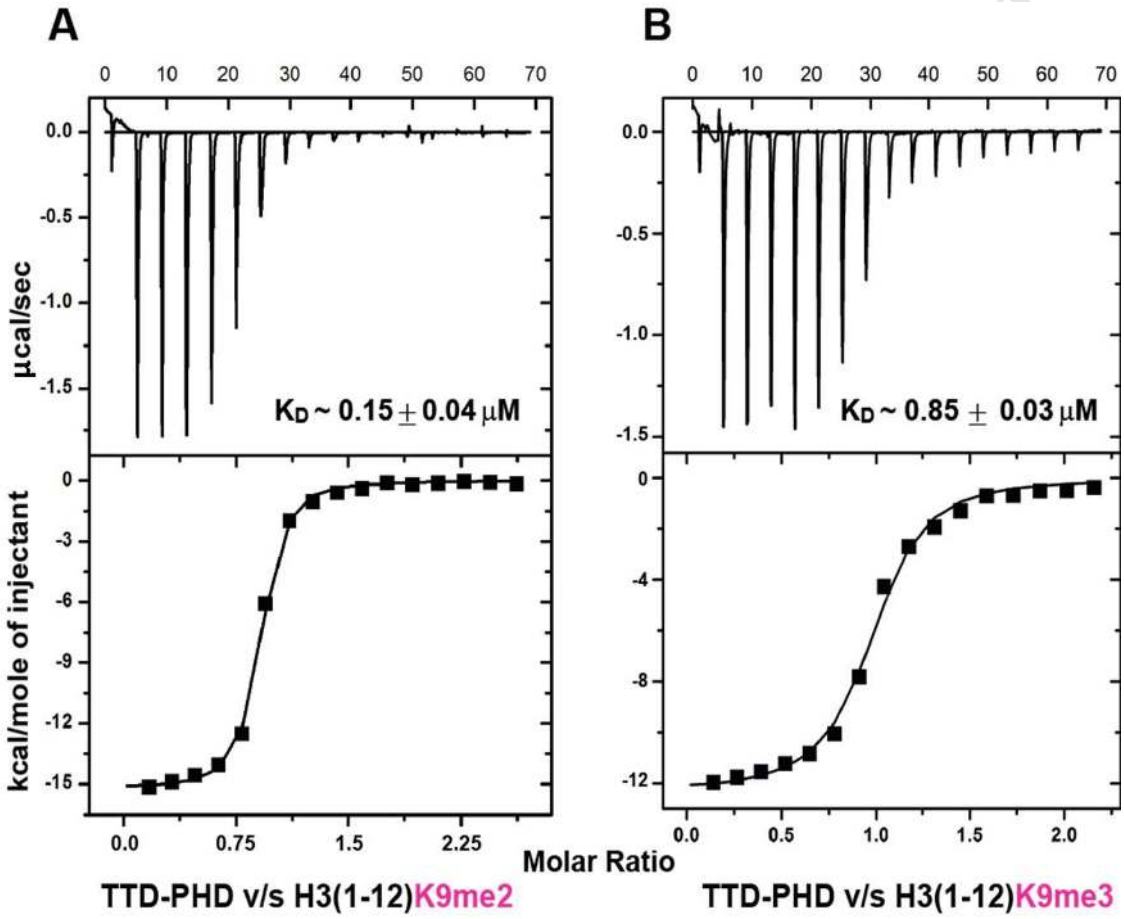

Fig. 4. ITC binding studies of H3R2K9me2 and H3R2K9me3 peptides to UHRF1 TTD-PHD cassette. Enthalpy plots for the binding of the UHRF1 TTD-PHD to (A) H3R2K9me2 and (B) H3R2K9me3 peptides. The inset lists the measured molar dissociation constant.

3.5. MD simulation studies on binding of H3K4me2K9me2 and H3K4me2K9me3 peptides to UHRF1 TTD-PHD Cassette

To gain insights into the effect of lysine 4 methylation on the combinatorial binding of H3K9me2/3 and H3R2 to the UHRF1 TTD-PHD, we have under taken MD

simulation studies on, energy minimized, TTD-PHD-H3(1-12)K4me2K9me2 and TTD-PHD-H3(1-12)K4me2K9me3 complexes. The dynamics of the intermolecular contacts between TTD-PHD and H3R2K4me2K9me2 peptide are similar to interactions observed between TTD-PHD and H3R2K9me2 (Fig. 3C and 5A). Similarly, H3R2K4me2K9me3 and H3R2K9me3 peptides have highly comparable intermolecular contacts with TTD-PHD (Fig. 3D and 5B). In addition, UHRF1 TTD-PHD has similar ΔG_{bind} towards H3R2K4me2K9me2 and H3R2K9me2 peptides. In line, H3R2K4me2K9me3 and H3R2K9me3 peptides also exhibit similar ΔG_{bind} towards UHRF1 TTD-PHD (Table 1). Further, H3R2K9me2 and H3R2K4me2K9me2 peptides show similar RMSFs (Supplementary Fig. 3A,B). Taken together, these studies suggest that methyl-lysine 4 has a negligible effect on recognition of H3R2K9me2/3 peptides by the UHRF1 TTD-PHD.

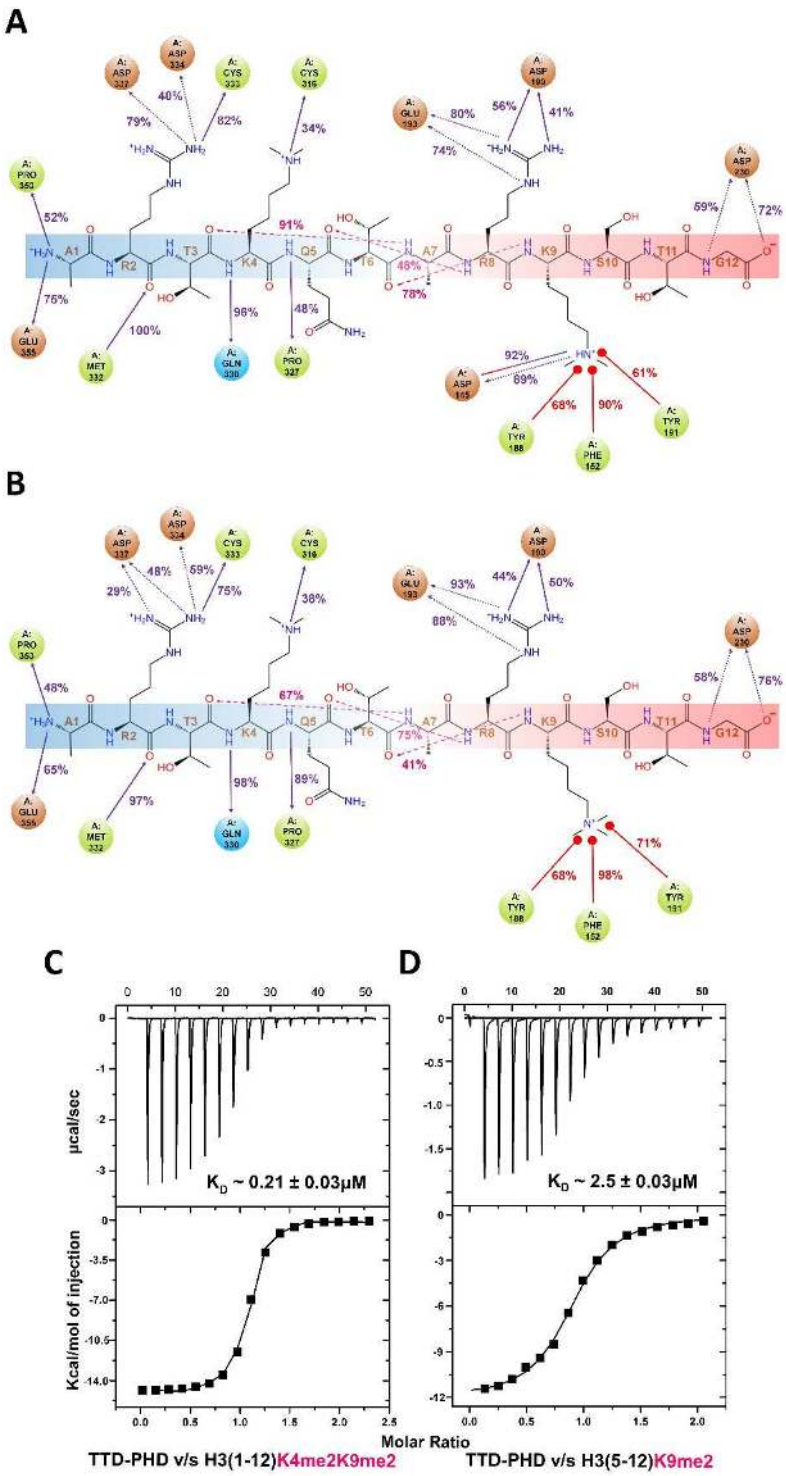

Fig. 5. The peptide-protein contacts during simulation time, and ITC binding studies of UHRF1 TTD-PHD to single- and dual- methylated lysine H3 peptides. 2D-interaction diagram of **UHRF1 TTD-PHD** to (A) H3K4me2K9me2 and (B)

H3K4me2K9me3 peptides. Enthalpy plots for the binding of the UHRF1 TTD-PHD to (C) H3K4me2K9me2 and (D) H3K9me2 peptides.

3.6. Dimethyl-lysine 4 on H3 has insignificant effect on H3R2K9me2 recognition by the UHRF1 TTD-PHD Cassette

To test MD simulation results, we carried out ITC binding study using the H3(1-12)K4me2K9me2 peptide and the UHRF1 TTD-PHD. UHRF1 TTD-PHD cassette binds dual lysine-methylated peptide, H3R2K4me2K9me2, with a K_D of 0.21 μM, which is similar to that of TTD-PHD binding to H3(1-12)R2K9me2 (Fig. 4A and 5C), thereby supporting the MD simulation results.

3.7. Effect of UHRF1 PHD domain on histone H3K9me2 recognition by the UHRF1 TTD

We have carried out ITC binding study to unravel the effect of UHRF1 PHD on H3K9me2 recognition by the TTD of UHRF1 in the context of TTD-PHD dual domains. Only first four residues (A1-R2-T3-K4) of H3 peptide are recognized by the PHD finger [5,16,17]. In contrast, residues 7-10 of histone H3 are recognized by the TTD domain of TTD-PHD in crystal structure [11]. Therefore, both PHD and TTD are required for recognition of H3(1-10)K9me. We have used 5-12 residues H3 peptide for binding study to rule out the contribution of PHD finger for K9me2 recognition. UHRF1 TTD-PHD binds H3(5-12)K9me2 peptide with a K_D of 2.5 μM (Fig. 5D), which is similar to H3(1-12)K9me2 peptide recognition by the UHRF1 TTD (Fig. 1C). Therefore, PHD finger has a minimal contribution for binding affinity to recognize K9me2 on H3 peptide by the UHRF1 TTD-PHD dual domain cassette.

4. Discussion

UHRF1 TTD as a stand-alone domain binds to H3K9me2 with a significantly higher binding affinity compared to H3K4me2, H3K27me2 and H4K20me2 (Fig 1C-F). It is possible that UHRF1 TTD can non-specifically bind other methyl-lysine, H3K4me2 and H3K27me2, marks in different sequence contexts. There has been a recent interest in and appreciation of multivalent or combinatorial readout of two or more histone marks by a corresponding number of ‘reader’ modules, highlighting its role in specific and

selective recognition of epigenetic marks at the histone and/or nucleosome level [42]. The linker (region 296-301) between PHD and TTD in UHRF1 might act as a ruler/spacer for simultaneous recognition of R2 and K9me2 on H3 in 'cis' context by dual domains [16]. Recognition of N-terminal amino group, Ala1 and Arg2 of H3 peptide by the PHD (Supplementary Fig. 1) [5] not only prevents the non-specific recognition of histone H3 methyl-lysines, such as H3K4me and H3K27me, by the TTD but also restricts TTD to recognize the H3K9me (Supplementary Fig. 1). Our hypothesis is supported by a previous study showing that UHRF1 TTD-PHD exhibits negligible binding affinity to trimethylated histone H3 lysine 27 or 36 peptides [17].

4.1. Effect of negatively charged residue in the binding pocket on lower methyl-lysine status recognition

The current study, on the role of Asp145 at the binding pocket for preferential recognition of K9me2 over K9me3 (Fig. 3, Table 1), is supported by the previous studies on lower methyl-lysine status-specific readout by MBT repeats of L3MBTL1 and 53BP1 TTD. Those studies reported that the presence of negatively charged residue in the aromatic cage binding pocket is linked to lower methyl-lysine status recognition of H1.4K26, H3K4, H3K9, H3K27, H3K36 or H4K20 peptides [11,43,44] (Fig. 1B and 6A). Substitution, of one of the aromatic cage residues in the binding pocket to the negatively charged residue (Asp/Glu), was used to engineer the PHD finger of BPTF and the Chromodomain of HP1α to preferentially bind dimethyl-lysine of histone H3 [43,45]. Furthermore, preferential recognition of H3K9me2 over H3K9me3 peptide by the UHRF1 TTD-PHD Asp145Glu mutant is highlighting the role of negatively charged residue for preferential recognition of lower methylation status (Supplementary Fig. 4). In contrast to the current study, the previous study reported that UHRF1 TTD preferentially binds H3K9me3 over H3K9me2 [9]. Use of N-terminal fluorophore labelled H3 peptide for binding study, that may affect the recognition of H3 peptide by the TTD, might be the reason for an anomaly in the previous study [9]. Fluorescent polarization binding studies using the C-terminal fluorescein labelled, H3(1-12)K9me2 and H3(1-12)K9me3, peptides validate the preferential recognition of H3K9me2 methylation status by the UHRF1 TTD (Supplementary Fig. 5).

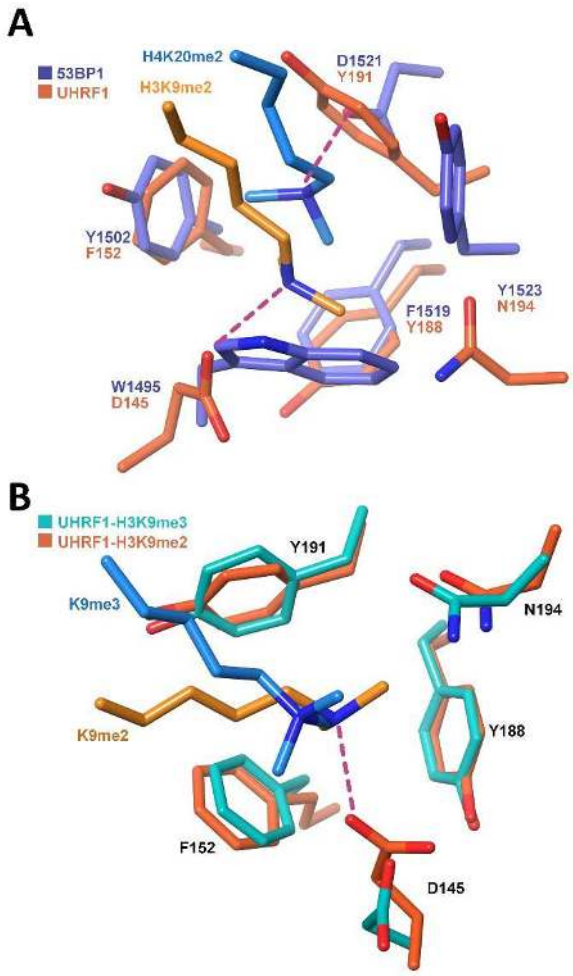

Fig. 6. Structural Comparison between UHRF1 TTD and 53BP1 TTD domains complexed to H3K9me2 and H4K20me2 peptides respectively.

(A) Superposition of MD simulated UHRF1 TTD-PHD-H3K9me2 complex structure on crystal structure of 53BP1 TTD-H4K20me2 complex. UHRF1 TTD (reddish-brown color) bound to H3K9me2 peptide (brown) and 53BP1 TTD (purple) bound to H4K20me2 peptide (blue) (PDB: 2IG0) are represented in stick. Intermolecular hydrogen bonds involving the dimethyl-ammonium group are shown by dashed pink lines both in panels A and B.

(B) Comparison of K9me3 and K9me2 recognition in the H3K9me binding pocket of UHRF1 TTD at the end of 10ns simulation of UHRF1 TTD-PHD-H3K9me2 and UHRF1 TTD-PHD-H3K9me3 complexes. Binding pocket of UHRF1 TTD (reddish-brown stick)

bound to K9me2 (brown stick) is superimposed on UHRF1 TTD (cyan stick) bound K9me3 (blue stick).

4.2. Comparison of methyl-lysine statuses recognition by the TTD domains of UHRF1 and 53BP1

A notable difference, in methyl-lysine recognition by the TTD of UHRF1 and of 53BP1, is that the UHRF1 TTD preferentially binds dimethyl status of H3K9me but 53BP1 TTD exhibits selectivity towards dimethyl status of H4K20me [11] (Fig. 1C and 2). To gain further insights into the above observation, we compared the structure of the 53BP1 TTD bound to the H4K20me2 peptide (PDB ID: 2IG0) to the, MD simulated, UHRF1 TTD-PHD-H3(1-12)K9me2 peptide complex (Fig. 6A). The dimethyl-lysine is bound in the pockets of the TUDOR1 domain, and dimethyl-ammonium proton is hydrogen-bonded to Asp side chain in both the complexes. The volume of the UHRF1 TTD (108.51 $Å^3$) methyl-lysine binding pocket is larger, because of three aromatic residues that surround the binding pocket, compared to 53BP1 TTD (87.5 $Å^3$), which has five aromatic residues (Fig. 1B and 6A). This may constrain the 53BP1 TTD to accommodate only dimethyl-lysine status (Fig. 6A).

4.3. Comparison of dynamics of the dimethyl-lysine 9 and the trimethyl-lysine 9 recognition by the UHRF1 TTD

To understand the dynamics of methyl-lysine statuses recognition by the UHRF1 TTD domain, we compared MD simulated structures of UHRF1 TTD-PHD-H3K9me2 complex with that of the UHRF1 TTD-PHD-H3K9me3 complex (Fig. 6B). Unlike 53BP1 TTD, UHRF1 TTD can accommodate both dimethyl-lysine and trimethyl-lysine statuses but prefers former over later (Fig. 6B). Conformations of dimethyl- and trimethyl-lysines, in the binding pocket, are such that only dimethyl-lysine has hydrogen bond interaction with the Asp145. Among binding pocket residues, Asp145 is moved towards the methyl-lysine in UHRF1 TTD-PHD-H3K9me2 complex, in contrast, it is moved away from the methyl-lysine in the UHRF1 TTD-PHD-H3K9me3 complex. Above conformational changes are necessary for preferential recognition of H3K9me2 over H3K9me3 and to avoid the exposure of one of the methyl groups to the negatively charged environment

that might weaken the recognition of trimethyl-lysine status by the UHRF1 TTD (Fig. 6B). UHRF1 TTD-PHD Asp145Glu mutant has significantly lower ΔG_{bind} for H3R2K9me2 peptide compared to H3R2K9me3 (Table 1). In contrast, UHRF1 TTD-PHD Asp145Ala mutant exhibits insignificant difference in ΔG_{bind} for above peptides (Table 1). These results corroborated the role of negatively charged residue, in the aromatic cage binding pocket, on preferential recognition of lower methylation status. Preferential recognition of H3K9me2 is supported by the global loss of H3K9me2 in the genome of embryonic stem cells (ESCs) that leads to loss of UHRF1 recruitment to chromatin [46].

Unbound N-terminus of histone H3 is unstructured [47]. However, the helical conformation of T3-T6 region of H3 peptide is required for combinatorial recognition of H3R2 and H3K9me2 by the TTD-PHD dual domains. Previously, it was reported that lysine 4 methylation on H3 decreases the binding affinity of human Survivin to H3T3 phosphorylation (H3T3ph) peptide [48]. Conversely, methylation of arginine 2 (H3R2me) is a critical epigenetic mark that antagonizes lysine 4 methylation (H3K4me) by blocking effector proteins binding through their reader domains [49,50]. Therefore, modification on this region may affect the recognition of the H3R2K9me2 peptide by the TTD-PHD cassette. In addition, methyl-lysine 4 on H3 may affect the hydrogen bond between the side chain of K4 and the main chain carboxyl group of the TTD-PHD dual domain [5,16,17]. Therefore, the presence of methyl groups in the polar surroundings might weaken H3R2K9me2 recognition by the UHRF1 TTD-PHD. However, MD simulation and binding studies indicate that dimethyl-lysine 4 neither affects the helical conformation of the peptide nor the combinatorial recognition of K9me2 and R2 marks by the TTD and PHD domains, respectively (Fig. 5A-C).

5. Conclusion

In this paper, we have characterized the histone methyl-lysine binding specificity of UHRF1 TTD. MD simulation and *in vitro* binding studies reveal that TTD, as standalone domain and also as PHD linked domain, preferentially binds H3K9me2 mark, and the UHRF1 PHD finger has an insignificant effect on K9me2 mark recognition by the UHRF1 TTD domain in the context of UHRF1 TTD-PHD cassette. Our results also demonstrate that post-translational modification, methylation of H3K4, does not

perturb the combinatorial recognition of H3R2 and H3K9me2 marks by the linked PHD and TUDOR domains of UHRF1.

In vitro binding analyses and/ or structural studies to determine the effect of post-translational modifications, residue substitution or functional group changes on the peptide or other ligands binding to receptor will be laborious and costly. Therefore, this study suggests that MD simulation on modeled protein-modified ligand complexes may give insights on the effect of such modifications on ligand binding. Results of such MD simulation studies can be the basis for further biochemical and structural characterization, and for the lead optimization in drug discovery process. In future, we plan to use MD simulation based structural analysis to identify the residues to engineer UHRF1 TTD-PHD to switch its methyl-lysine status binding specificity. The engineered UHRF1 module can be used to address the effect of a change in methyl-lysine status binding specificity on UHRF1's functions, in vivo, such as heterochromatin formation, DNA repair, cell proliferation, and stem cell self-renewal and differentiation.

Acknowledgements

M.A.N, N.K.N and E.R. thank Dr. Sanjeev Khosla and Director, Centre for DNA Fingerprinting and Diagnostics (CDFD) for hosting at CDFD. We are grateful to Director, CSIR-Centre for Cellular & Molecular Biology for providing access to the ITC instrument. The authors are grateful to Dr. Usha Nagarajan, Department of BioEngineering, School of Chemical and Biotechnology, SASTRA University, Thanjavur, Tamil Nadu, and to Dr. Sandeep Kumar Singh, Department of Biotechnology, IIT Hyderabad, India for critical reading of the manuscript.

Competing Interests

The Authors declare that there are no competing interests associated with the manuscript.

Funding

S.A. and M.A.N. are supported by research fellowships from the Ministry of Human Resource Development, Government of India. N.K.N. and W.D. thank the University Grant Commission, Government of India for the fellowship. S.K. was supported by fund from Department of Biotechnology (DBT), Govt of India. E.R. thanks

the DBT and the Science and Engineering Research Board, Govt of India for the Ramalingaswami Re-entry fellowship and Early Career Research Award. E.R. research is supported by fund from the DBT and the Indian Institute of Technology Hyderabad.

References:

[1] Taverna SD, Li H, Ruthenburg AJ, Allis CD, Patel DJ. How chromatin-binding modules interpret histone modifications: lessons from professional pocket pickers. Nat Struct Mol Biol. 2007 Nov;14(11):1025–40.

[2] Bostick M, Kim JK, Estève P-O, Clark A, Pradhan S, Jacobsen SE. UHRF1 plays a role in maintaining DNA methylation in mammalian cells. Science. 2007 Sep 21;317(5845):1760–4.

[3] Sharif J, Muto M, Takebayashi S, Suetake I, Iwamatsu A, Endo TA, et al. The SRA protein Np95 mediates epigenetic inheritance by recruiting Dnmt1 to methylated DNA. Nature. 2007 Dec 6;450(7171):908–12.

[4] Karagianni P, Amazit L, Qin J, Wong J. ICBP90, a novel methyl K9 H3 binding protein linking protein ubiquitination with heterochromatin formation. Mol Cell Biol. 2008 Jan;28(2):705–17.

[5] Rajakumara E, Wang Z, Ma H, Hu L, Chen H, Lin Y, et al. PHD finger recognition of unmodified histone H3R2 links UHRF1 to regulation of euchromatic gene expression. Mol Cell. 2011 Jul 22;43(2):275–84.

[6] Papait R, Pistore C, Grazini U, Babbio F, Cogliati S, Pecoraro D, et al. The PHD domain of Np95 (mUHRF1) is involved in large-scale reorganization of pericentromeric heterochromatin. Mol Biol Cell. 2008 Aug;19(8):3554–63.

[7] Hu L, Li Z, Wang P, Lin Y, Xu Y. Crystal structure of PHD domain of UHRF1 and insights into recognition of unmodified histone H3 arginine residue 2. Cell Res. 2011 Sep;21(9):1374–8.

[8] Wang C, Shen J, Yang Z, Chen P, Zhao B, Hu W, et al. Structural basis for site-specific reading of unmodified R2 of histone H3 tail by UHRF1 PHD finger. Cell Res. 2011 Aug 2;21(9):cr2011123.

[9] Nady N, Lemak A, Walker JR, Avvakumov GV, Kareta MS, Achour M, et al. Recognition of Multivalent Histone States Associated with Heterochromatin by UHRF1 Protein. J Biol Chem. 2011 Jul 8;286(27):24300–11.

[10] Xie S, Jakoncic J, Qian C. UHRF1 double tudor domain and the adjacent PHD finger act together to recognize K9me3-containing histone H3 tail. J Mol Biol. 2012 Jan 13;415(2):318–28.

[11] Botuyan MV, Lee J, Ward IM, Kim J-E, Thompson JR, Chen J, et al. Structural basis for the methylation state-specific recognition of histone H4-K20 by 53BP1 and Crb2 in DNA repair. Cell. 2006 Dec 29;127(7):1361–73.

[12] Charier G, Couprie J, Alpha-Bazin B, Meyer V, Quéméneur E, Guérois R, et al. The Tudor tandem of 53BP1: a new structural motif involved in DNA and RG-rich peptide binding. Struct Lond Engl 1993. 2004 Sep;12(9):1551–62.

[13] Roy S, Musselman CA, Kachirskaia I, Hayashi R, Glass KC, Nix JC, et al. Structural insight into p53 recognition by the 53BP1 tandem Tudor domain. J Mol Biol. 2010 May 14;398(4):489–96.

[14] Tong Q, Cui G, Botuyan MV, Rothbart SB, Hayashi R, Musselman CA, et al. Structural plasticity of methyllysine recognition by the tandem tudor domain of 53BP1. Struct Lond Engl 1993. 2015 Feb 3;23(2):312–21.

[15] Carr SM, Munro S, Zalmas L-P, Fedorov O, Johansson C, Krojer T, et al. Lysine methylation-dependent binding of 53BP1 to the pRb tumor suppressor. Proc Natl Acad Sci U S A. 2014 Aug 5;111(31):11341–6.

[16] Arita K, Isogai S, Oda T, Unoki M, Sugita K, Sekiyama N, et al. Recognition of modification status on a histone H3 tail by linked histone reader modules of the epigenetic regulator UHRF1. Proc Natl Acad Sci U S A. 2012 Aug 7;109(32):12950–5.

[17] Cheng J, Yang Y, Fang J, Xiao J, Zhu T, Chen F, et al. Structural insight into coordinated recognition of trimethylated histone H3 lysine 9 (H3K9me3) by the plant homeodomain (PHD) and tandem tudor domain (TTD) of UHRF1 (ubiquitin-like, containing PHD and RING finger domains, 1) protein. J Biol Chem. 2013 Jan 11;288(2):1329–39.

[18] Rothbart SB, Dickson BM, Ong MS, Krajewski K, Houliston S, Kireev DB, et al. Multivalent histone engagement by the linked tandem Tudor and PHD domains of UHRF1 is required for the epigenetic inheritance of DNA methylation. Genes Dev. 2013 Jun 1;27(11):1288–98.

[19] Fang J, Cheng J, Wang J, Zhang Q, Liu M, Gong R, et al. Hemi-methylated DNA opens a closed conformation of UHRF1 to facilitate its histone recognition. Nat Commun. 2016 Apr 5;7:ncomms11197.

[20] Rajakumara E, Nakarakanti NK, Nivya MA, Satish M. Mechanistic insights into the recognition of 5-methylcytosine oxidation derivatives by the SUVH5 SRA domain. Sci Rep. 2016 Feb 4;6:20161.

[21] Rajakumara E, Law JA, Simanshu DK, Voigt P, Johnson LM, Reinberg D, et al. A dual flip-out mechanism for 5mC recognition by the Arabidopsis SUVH5 SRA domain and its impact on DNA methylation and H3K9 dimethylation in vivo. Genes Dev. 2011 Jan 15;25(2):137–52.

[22] Arita K, Ariyoshi M, Tochio H, Nakamura Y, Shirakawa M. Recognition of hemi-methylated DNA by the SRA protein UHRF1 by a base-flipping mechanism. Nature. 2008 Oct 9;455(7214):818–21.

[23] Avvakumov GV, Walker JR, Xue S, Li Y, Duan S, Bronner C, et al. Structural basis for recognition of hemi-methylated DNA by the SRA domain of human UHRF1. Nature. 2008 Oct 9;455(7214):822–5.

[24] Hashimoto H, Horton JR, Zhang X, Bostick M, Jacobsen SE, Cheng X. The SRA domain of UHRF1 flips 5-methylcytosine out of the DNA helix. Nature. 2008 Oct 9;455(7214):826–9.

[25] Qian C, Li S, Jakoncic J, Zeng L, Walsh MJ, Zhou M-M. Structure and hemimethylated CpG binding of the SRA domain from human UHRF1. J Biol Chem. 2008 Dec 12;283(50):34490–4.

[26] Rottach A, Frauer C, Pichler G, Bonapace IM, Spada F, Leonhardt H. The multi-domain protein Np95 connects DNA methylation and histone modification. Nucleic Acids Res. 2010 Apr;38(6):1796–804.

[27] Zhou VW, Goren A, Bernstein BE. Charting histone modifications and the functional organization of mammalian genomes. Nat Rev Genet. 2011 Jan;12(1):7–18.

[28] Wang Y, Li X, Hu H. H3K4me2 reliably defines transcription factor binding regions in different cells. Genomics. 2014 Mar;103(2–3):222–8.

[29] Heintzman ND, Stuart RK, Hon G, Fu Y, Ching CW, Hawkins RD, et al. Distinct and predictive chromatin signatures of transcriptional promoters and enhancers in the human genome. Nat Genet. 2007 Mar;39(3):311–8.

[30] Santos-Rosa H, Schneider R, Bannister AJ, Sherriff J, Bernstein BE, Emre NCT, et al. Active genes are tri-methylated at K4 of histone H3. Nature. 2002 Sep 26;419(6905):407–11.

[31] Li H, Ilin S, Wang W, Duncan EM, Wysocka J, Allis CD, et al. Molecular basis for site-specific read-out of histone H3K4me3 by the BPTF PHD finger of NURF. Nature. 2006 Jul 6;442(7098):91–5.

[32] Winter S, Fischle W. Epigenetic markers and their cross-talk. Essays Biochem. 2010 Sep 20;48(1):45–61.

[33] Vaissière T, Herceg Z. Histone code in the cross-talk during DNA damage signaling. Cell Res. 2010 Feb;20(2):113–5.

[34] Winter S, Simboeck E, Fischle W, Zupkovitz G, Dohnal I, Mechtler K, et al. 14-3-3 proteins recognize a histone code at histone H3 and are required for transcriptional activation. EMBO J. 2008 Jan 9;27(1):88–99.

[35] Wang Z, Patel DJ. Combinatorial readout of dual histone modifications by paired chromatin-associated modules. J Biol Chem. 2011 May 27;286(21):18363–8.

[36] Bas DC, Rogers DM, Jensen JH. Very fast prediction and rationalization of pKa values for protein-ligand complexes. Proteins. 2008 Nov 15;73(3):765–83.

[37] Li H, Robertson AD, Jensen JH. Very fast empirical prediction and rationalization of protein pKa values. Proteins. 2005 Dec 1;61(4):704–21.

[38] Darden T, York D, Pedersen L. Particle mesh Ewald: An N·log(N) method for Ewald sums in large systems. J Chem Phys. 1993 Jun 15;98(12):10089–92.

[39] Hoover WG. Canonical dynamics: Equilibrium phase-space distributions. Phys Rev A. 1985 Mar 1;31(3):1695–7.

[40] Martyna GJ, Tobias DJ, Klein ML. Constant pressure molecular dynamics algorithms. J Chem Phys. 1994 Sep 1;101(5):4177–89.

[41] Rastelli G, Del Rio A, Degliesposti G, Sgobba M. Fast and accurate predictions of binding free energies using MM-PBSA and MM-GBSA. J Comput Chem. 2010 Mar;31(4):797–810.

[42] Ruthenburg AJ, Li H, Patel DJ, Allis CD. Multivalent engagement of chromatin modifications by linked binding modules. Nat Rev Mol Cell Biol. 2007 Dec;8(12):983–94.

[43] Li H, Fischle W, Wang W, Duncan EM, Liang L, Murakami-Ishibe S, et al. Structural basis for lower lysine methylation state-specific readout by MBT repeats of L3MBTL1 and an engineered PHD finger. Mol Cell. 2007 Nov 30;28(4):677–91.

[44] Min J, Allali-Hassani A, Nady N, Qi C, Ouyang H, Liu Y, et al. L3MBTL1 recognition of mono- and dimethylated histones. Nat Struct Mol Biol. 2007 Dec;14(12):1229–30.

[45] Eisert RJ, Waters ML. Tuning HP1α chromodomain selectivity for di- and trimethyllysine. Chembiochem Eur J Chem Biol. 2011 Dec 16;12(18):2786–90.

[46] von Meyenn F, Iurlaro M, Habibi E, Liu NQ, Salehzadeh-Yazdi A, Santos F, et al. Impairment of DNA Methylation Maintenance Is the Main Cause of Global Demethylation in Naive Embryonic Stem Cells. Mol Cell. 2016 Jun 16;62(6):848–61.

[47] Luger K, Mäder AW, Richmond RK, Sargent DF, Richmond TJ. Crystal structure of the nucleosome core particle at 2.8 Å resolution. Nature. 1997 Sep;389(6648):251–60.

[48] Du J, Kelly AE, Funabiki H, Patel DJ. Structural Basis for Recognition of H3T3ph and Smac/DIABLO N-terminal Peptides by Human Survivin. Structure. 2012 Jan 11;20(1):185–95.

[49] Kirmizis A, Santos-Rosa H, Penkett CJ, Singer MA, Vermeulen M, Mann M, et al. Arginine methylation at histone H3R2 controls deposition of H3K4 trimethylation. Nature. 2007 Oct;449(7164):928–32.

[50] Iberg AN, Espejo A, Cheng D, Kim D, Michaud-Levesque J, Richard S, et al. Arginine Methylation of the Histone H3 Tail Impedes Effector Binding. J Biol Chem. 2008 Feb 8;283(6):3006–10.

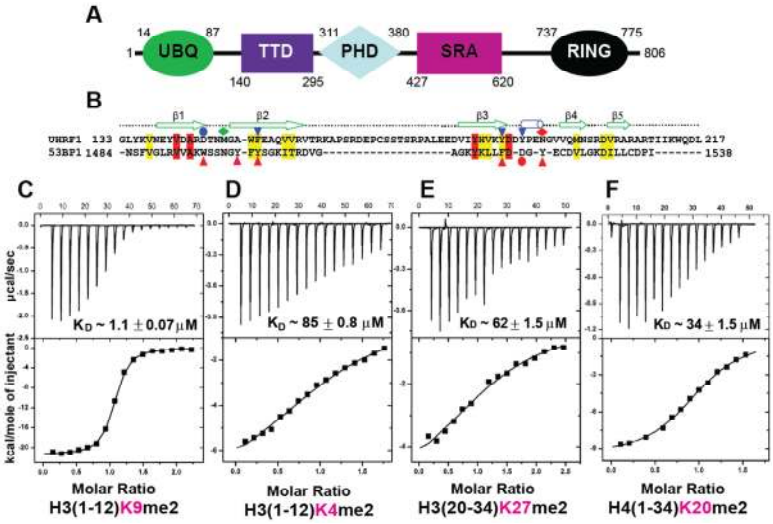

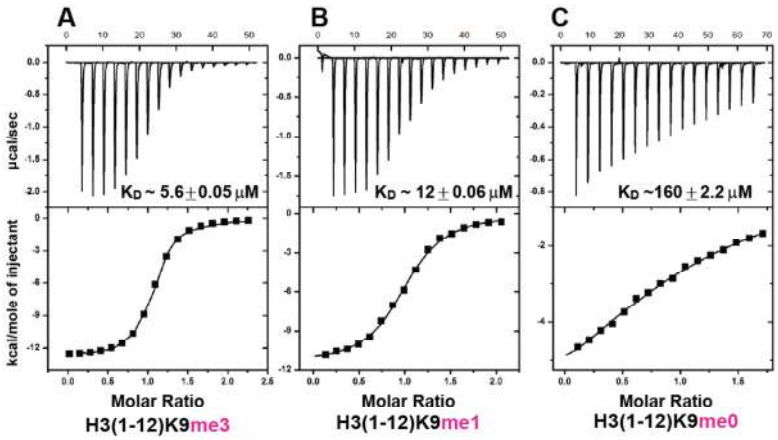

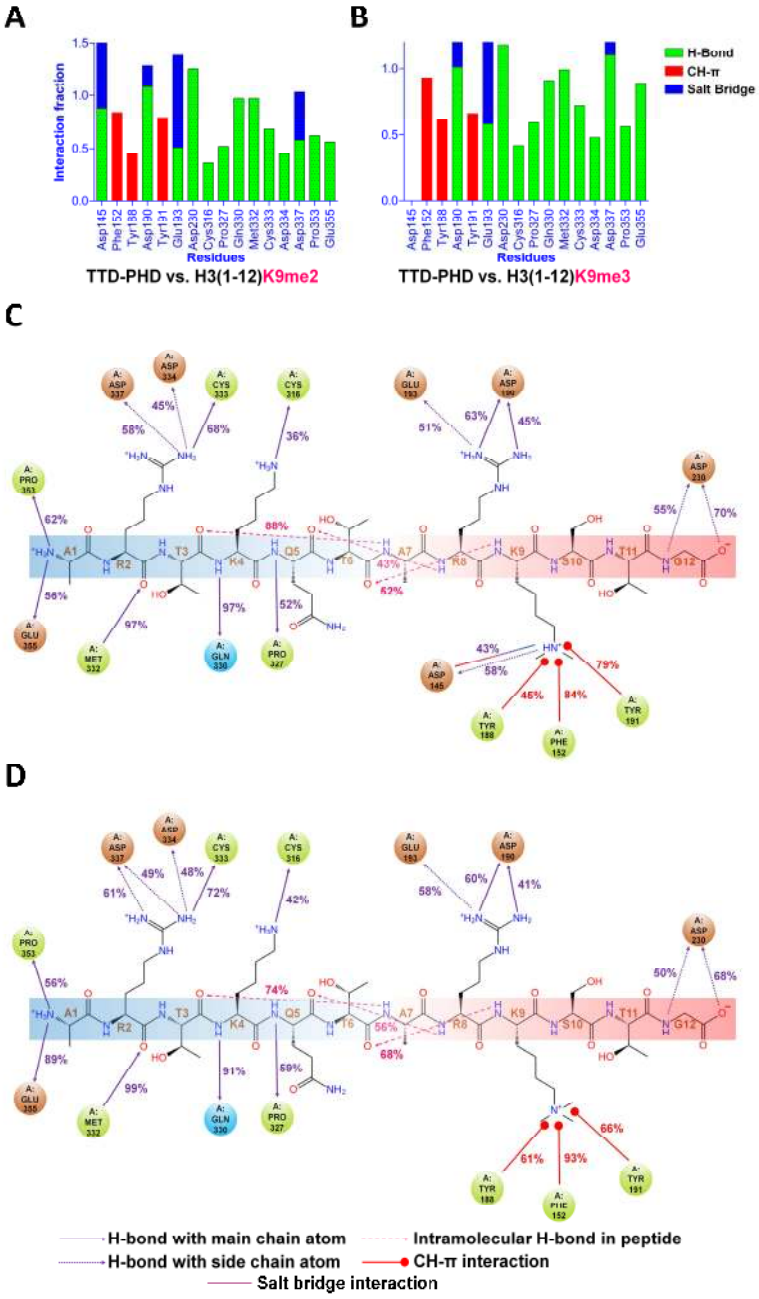
A
B
H-Bond
CH-π
Salt Bridge
Interaction fraction
Residues
Asp145 Phe152 Tyr188 Asp190 Tyr191 Glu193 Asp230 Cys316 Pro327 Gln330 Met332 Cys333 Asp334 Asp337 Pro353 Glu355
TTD-PHD vs. H3(1-12)K9me2
TTD-PHD vs. H3(1-12)K9me3
C
D
H-bond with main chain atom
H-bond with side chain atom
Salt bridge interaction
Intramolecular H-bond in peptide
CH-π interaction

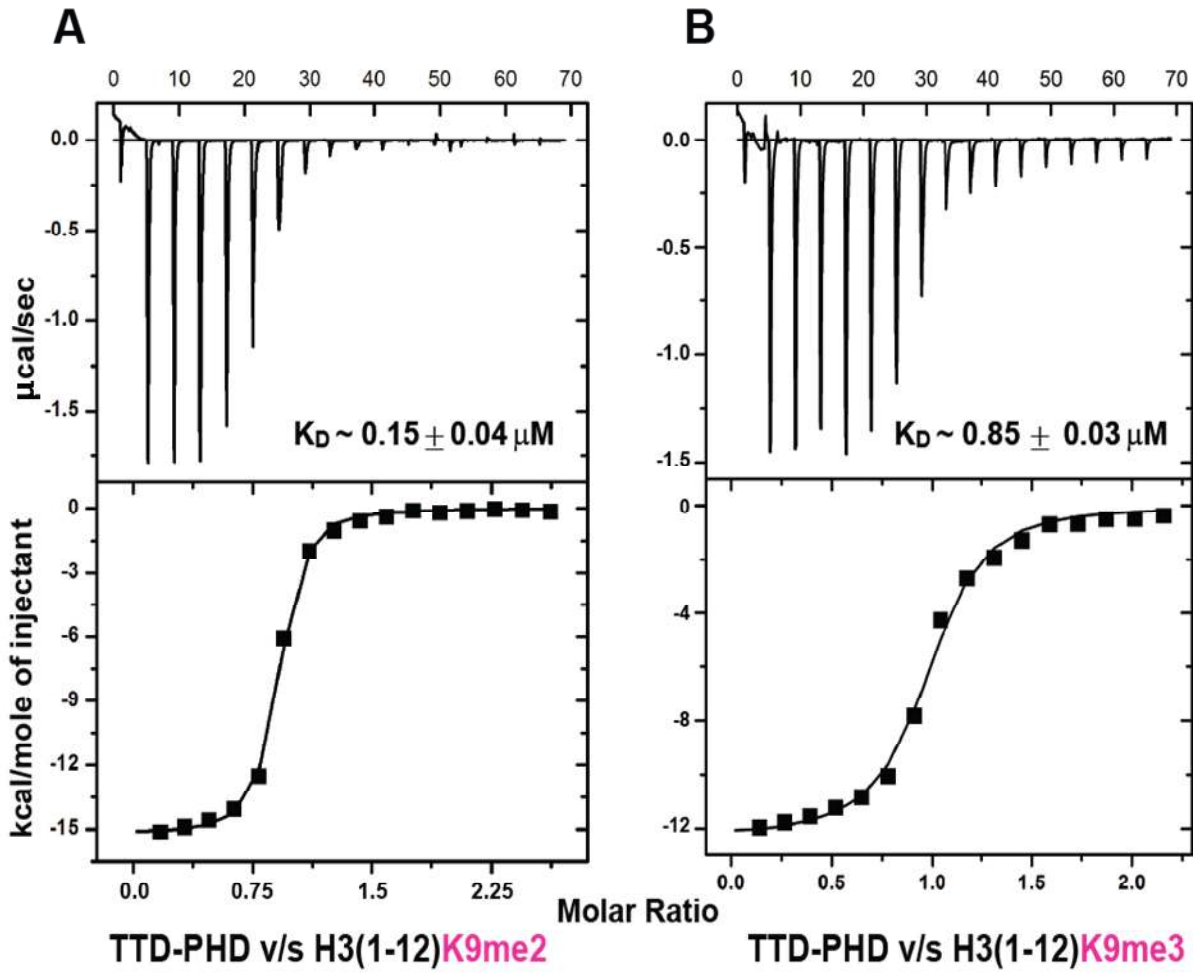
A
B
µcal/sec
kcal/mole of injectant
K_D ~ 0.15 ± 0.04 µM
K_D ~ 0.85 ± 0.03 µM
Molar Ratio
TTD-PHD v/s H3(1-12)K9me2
TTD-PHD v/s H3(1-12)K9me3

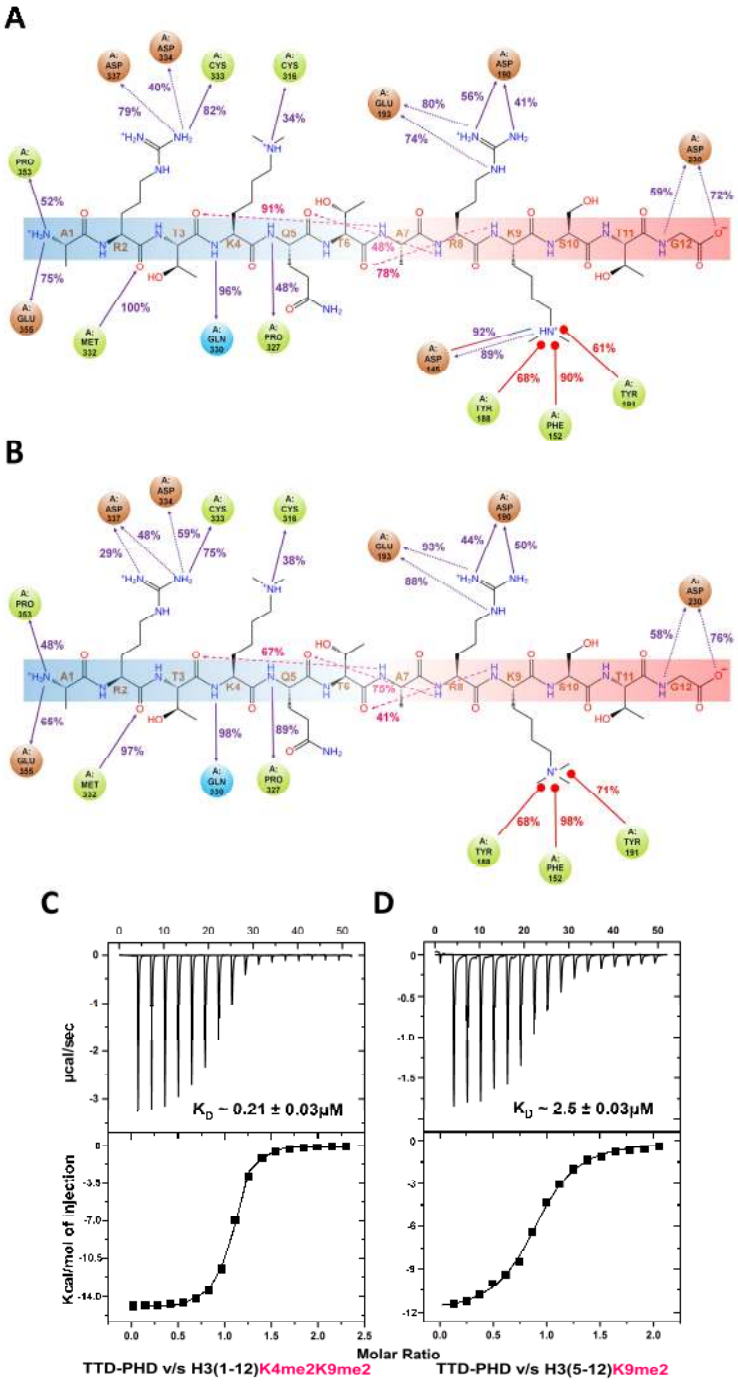
A
B
C
D
µcal/sec
Kcal/mol of injection
Molar Ratio
K_D ~ 0.21 ± 0.03µM
K_D ~ 2.5 ± 0.03µM
TTD-PHD v/s H3(1-12)K4me2K9me2
TTD-PHD v/s H3(5-12)K9me2

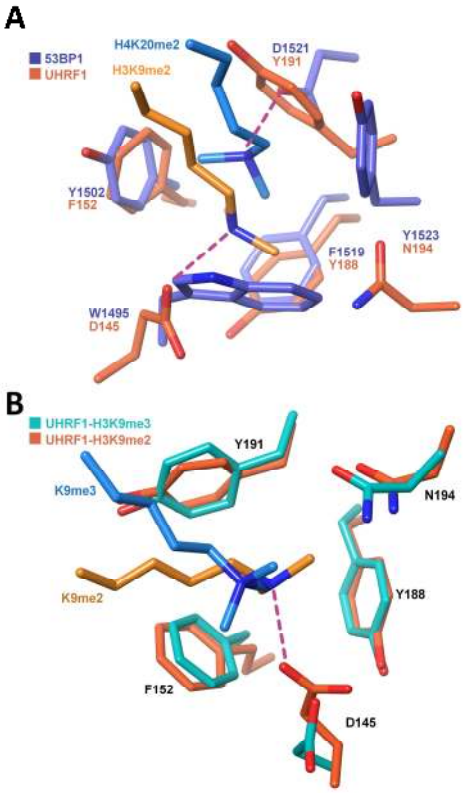

- Dynamic and binding specificity of histone H3 methyllysine peptides to UHRF1 presented
- UHRF1 TTD-PHD recognizes all methyl-lysine statuses of H3K9me
- UHRF1 TTD-PHD preferentially binds H3K9me2
- Asp145 in the binding pocket determines the preferential binding of H3K9me2
- No effect of H3K4me2 on combinatorial recognition of H3R2 and H3K9me2 by UHRF1 TTD-PHD